

Orbit Processing and Analysis of a GEO Class of High Area-to-Mass Ratio Debris Objects

Tom Kelecy, Ray Deiotte and John Africano

Boeing LTS / AMOS, Kihei, HI and Colorado Springs, CO

Gene Stansbery

NASA JSC-KX, Houston, TX

Tim Payne

Air Force Space Command / A9AC, Colorado Springs, CO

ABSTRACT

A population of recently discovered deep space objects [1] is thought to be debris having origins from sources in the geosynchronous orbit (GEO) belt. Observations have been presented indicating that these objects have a high area-to-mass (A/m) ratio (1's to 10's of m^2/kg), and thus would explain the observed migration of eccentricity (0.1-0.6) and inclination that distinguishes their orbital characteristics. There is a heightened interest in the international community due to the large number and small size of these objects, as they pose a hazard to active satellites operating in the vicinity of the GEO belt. Observational coverage of these objects has been limited by the orbital phasing and the locations of the tracking sites. Boeing, NASA and the Air Force Space Command (AFSPC) have embarked on a collaborative effort with the Inter-Agency Space Debris Coordination Committee (IADC) to track selected high A/m of this population to more accurately characterize their orbits and orbit histories. Space Command tracking assets were tasked to provide angles measurements for representative set of 6 high A/m objects, and the data were used to establish a process for doing orbit updates that would accommodate *a priori* two-line element sets that will eventually be provided by the IADC. This paper presents the development and validation of the data processing and orbit update implementation, and preliminary analysis results of the high A/m class of objects. Limitations in the observational geometry, along with the apparent time variations in the nominal A/m values of some of the objects, pose a challenge for the orbit prediction. The ultimate goal is to establish a process that will provide long-term, relatively accurate orbital histories for these high A/m objects derived from a global set of observation metrics, and to capture photometric measurements when possible that will support characterization of these objects.

1. INTRODUCTION

A class of debris objects in the neighborhood of the geosynchronous (GEO) orbit belt has been under study in recent years [1]. The unique high area-to-mass ratio (A/m) of these objects makes them sensitive to solar radiation pressure effects. Though they have likely originated in GEO and GEO transfer orbits as the result of injection of objects into the GEO belt, the solar radiation pressure perturbations have caused the mean orbit parameters of these objects to evolve over time, in particular in inclination and eccentricity. The migration and orbital phasing make them a challenge to track and study from any one location on Earth.

The discovery of these objects and their proximity to the GEO belt has brought an awareness of the potential hazard to operational satellites. The international space debris community has agreed to collaborate in observing these objects in an attempt to characterize their physical properties, and to develop a database from which the orbital histories can be cataloged. Because of the challenges inherent in tracking and prediction of these objects, a set of processes and infrastructure needs to be developed that will allow seamless tracking of this class of objects. The AFSPC, Boeing, NASA and the IADC are building a collaboration that will support this.

High A/m objects of interest that are tracked by IADC resources produce TLE state vectors for those objects. A "handoff" process needs to be developed that allows these TLEs to be passed to AFSPC acquire and track. The work described in this paper supports the collaboration by exercising an orbit determination (OD) process that produces state vector estimates and predictions that can then be passed back to IADC observing resources to help insure continuity of tracking. The output products consist of both TLEs and osculating state vectors predicted out to 7-10 days, and reported at 1-day increments over that interval. However, this is flexible and will likely vary for each

object, and will be dictated by the observation phasing and orbital dynamic factors. Other work has been done that examines the challenges inherent in the handoff process [2, 3].

The OD processing of the AFSPC angles observations for a trial set of high area-to-mass (A/m) objects is described. In section 2 a set of 6 high A/m objects that were selected and used to develop the process are described. This includes orbit characteristics, and representative orbital histories that would be anticipated for such objects. The OD processing and subsequent prediction process is described in section 3 of this paper. Finally, in section 4 the OD analysis results are presented, and include anticipated prediction accuracies.

2. HIGH A/M TEST OBJECT CHARACTERISTICS

Observation data for six trial objects was provided by AFSPC. The data consisted of angular right ascension (RA) and declination (DEC) for the objects tracked from Space Surveillance Network (SSN) sensors located at Maui, Diego Garcia and Socorro. The nominal orbit parameters for the six objects are given in Table 1, along with the A/m values, and ground track repeat cycle in days. The A/m values range from 1 m²/kg to a little over 13 m²/kg, and the ground track phasing period ranges from 8 to 40 days. Note, this last metric is the time for each object to drift 360° in longitude around the fixed Earth, and so the time between periods of visibility from any given site will be something less than the cycle period provided. Inclinations range from 13.4° to 21.9°, while eccentricities vary from 0.02 to about 0.15.

OBJ#	EPOCH	SMA (KM)	ECC	INC (DEG)	RAAN (DEG)	AP (DEG)	MA (DEG)	A/M (M ² /KG)	RCY (DAYS)
4	2005/08/10 00:00:00	44487.0026	0.035754	21.9230	310.9248	279.6327	333.5213	13.0619	13.0000
5	2005/10/28 00:00:00	41349.8045	0.058336	13.6359	6.0610	241.2404	359.3945	2.2836	34.0000
6	2006/02/01 00:00:00	41380.0348	0.018833	13.3599	356.0653	214.0008	69.4076	2.2218	36.0000
7	2206/05/01 00:00:00	41466.8652	0.019243	13.6181	356.0123	102.8722	348.8483	1.0191	40.0000
8	2006/04/16 00:00:00	46225.0263	0.147406	18.6178	1.0254	7.9804	147.4371	5.7977	8.0000
9	2006/03/01 00:00:00	44621.1861	0.115467	18.8863	14.1388	347.8828	204.7765	2.0179	12.0000

Table 1. Nominal Keplerian Orbital Elements for Six High A/m Objects

An orbit and ground trace visualization of the six objects is shown in Fig. 1.a-b, where the ground traces represent orbits propagated over one repeat cycle. The Obj#4, Obj#8 and Obj#9 satellites have an east to west drift, while Obj#5, Obj#6 and Obj#7 drift west to east over the course of their respective drift cycles.

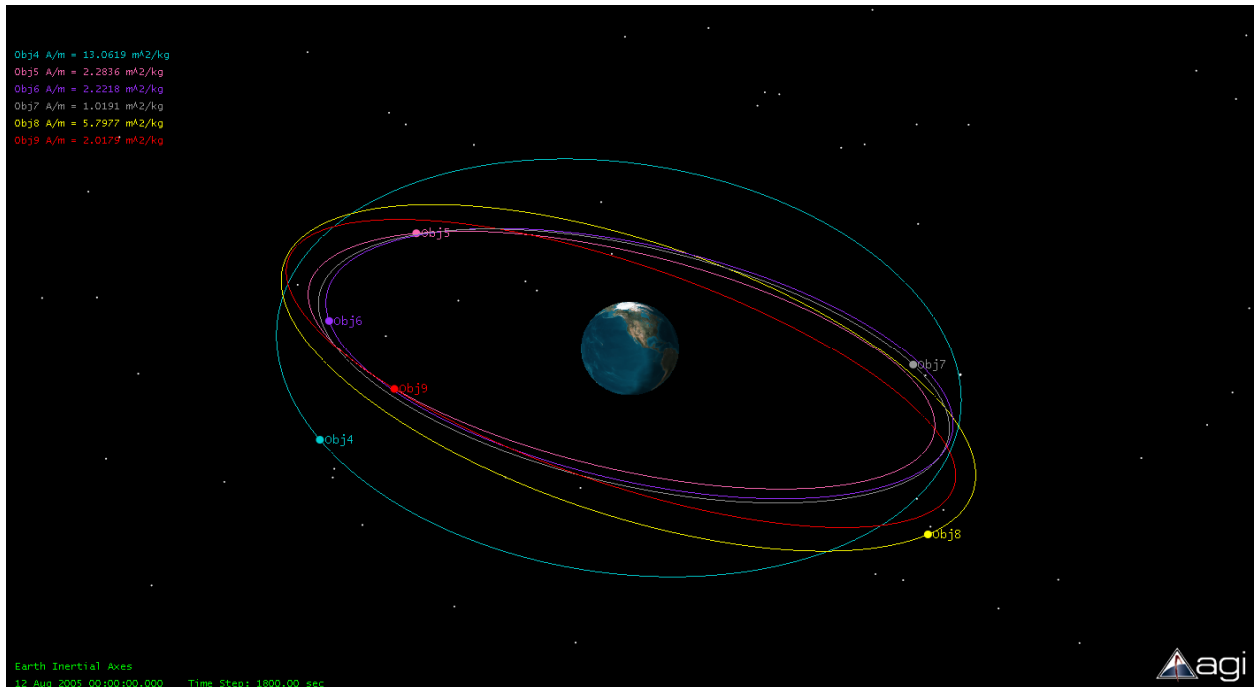


Fig. 1.a 3-Dimensional Visualization for Six Trial High A/m Objects

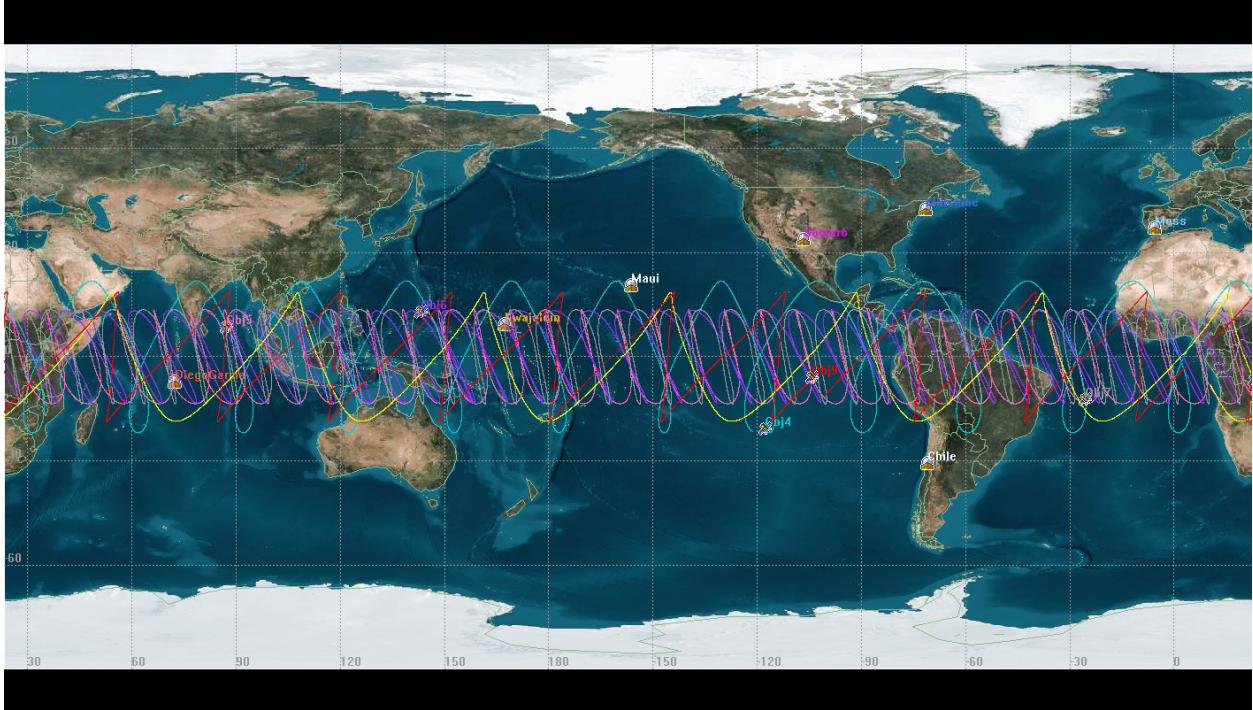


Fig. 1. 2-Dimensional Ground Trace Visualization for Six Trial High A/m Objects

One can use long-term propagation models to anticipate how the elements of these objects might evolve over an extended period of time as the result of solar radiation pressure, and other perturbations. Four fictitious GEO objects were propagated over a 20 year period, where the objects were given A/m values of $0.01 \text{ m}^2/\text{kg}$, $1 \text{ m}^2/\text{kg}$, $10 \text{ m}^2/\text{kg}$ and $20 \text{ m}^2/\text{kg}$, respectively. The 20 year histories for deviations from GEO period, eccentricity and inclination are shown in the Figures 2.a-c for each of the four A/m cases. The plot in Fig. 2.a shows the deviation from a GEO orbit period grows from 0 to nearly 15 minutes with increasing A/m. The inclination perturbation for each object is periodic with an amplitude that grows from 0° to about 32° , with the cycle period getting shorter with increasing A/m (period ~ 40 years for $A/m = 20 \text{ m}^2/\text{kg}$). The eccentricity perturbation amplitude varies from 0-0.5 with increasing A/m, and has a dominant annual periodicity for all of the A/m cases.

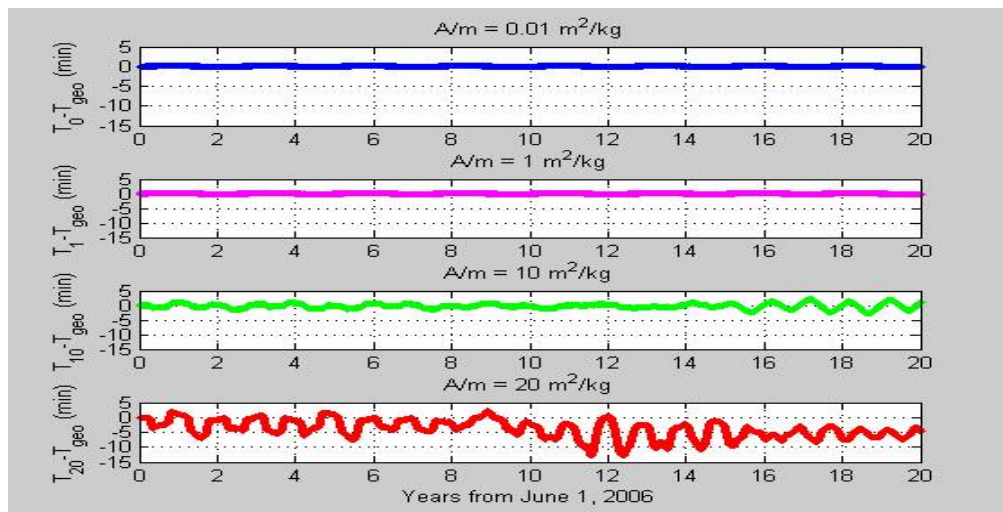


Fig. 2.a. Deviation from GEO Period 20-year Histories for $A/m = .01, 1, 10$ and $20 \text{ m}^2/\text{kg}$

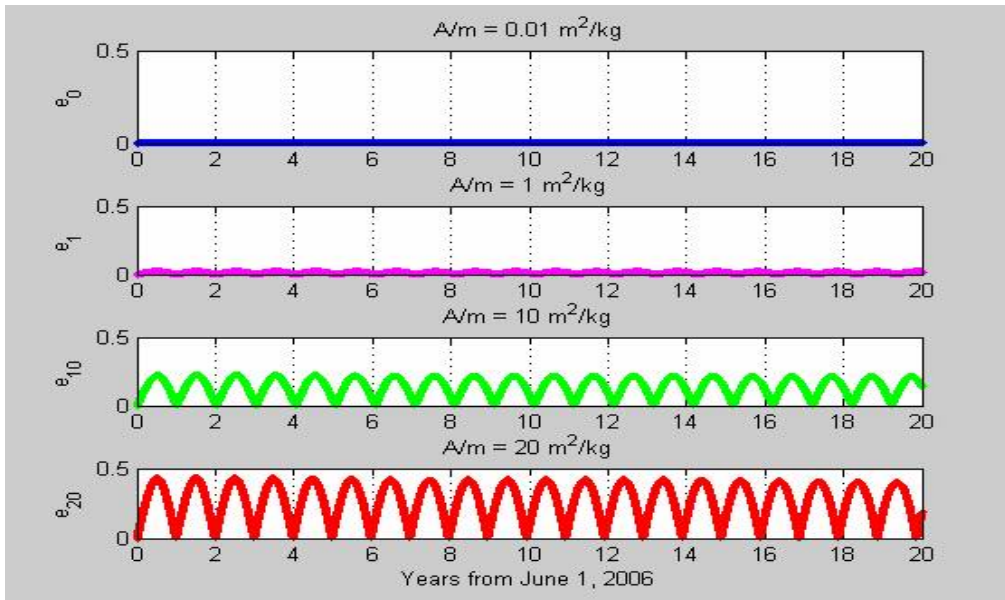


Fig. 2.b. Eccentricity 20-year Histories for $A/m = .01, 1, 10$ and $20 \text{ m}^2/\text{kg}$

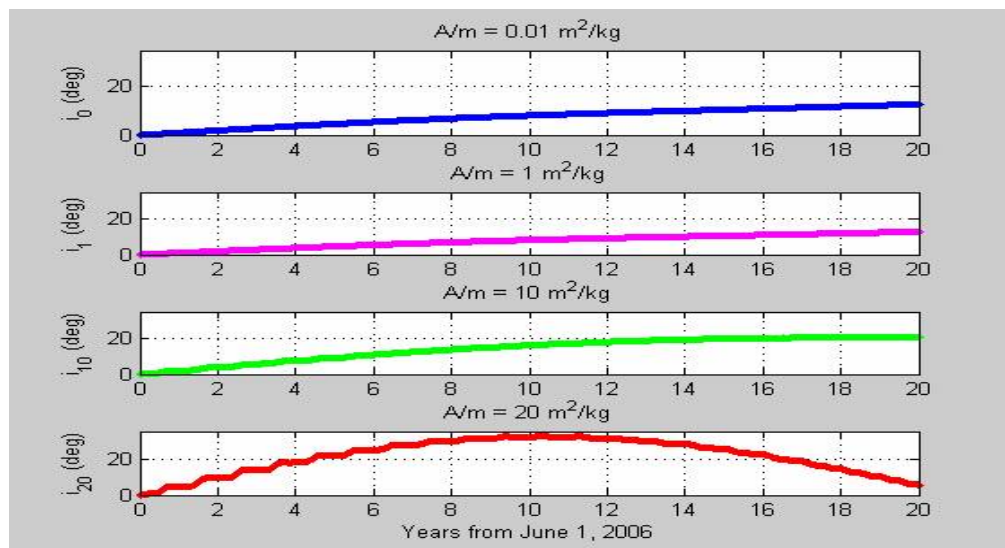


Fig. 2.c. Inclination 20-year Histories for $A/m = .01, 1, 10$ and $20 \text{ m}^2/\text{kg}$

One can anticipate from these theoretical results that the eccentricities and inclinations vary only slightly for the trial objects having A/m 1-3 m^2/kg . The trial objects have A/m values of $\sim 5 \text{ m}^2/\text{kg}$ and $\sim 13 \text{ m}^2/\text{kg}$ should show more significant variation of eccentricity and inclination over time, and should be measurable if the objects are tracked regularly over the course of a year. The observational data analyzed for the six high A/m objects covers a period ranging from 3 to 11 months. It should be noted that there are periods of time where data quality is poor, and that the periods include some data outages resulting from the natural longitudinal drift of the objects relative to the tracking site.

3. ORBIT DETERMINATION PROCESSING AND ORBIT PREDICTION

An OD process was developed to provide high A/m object tracking and prediction products that could be used to support acquisition and tracking by international collaborators. The orbital dynamics result in observation phasing that truly requires continuous global coverage to insure that the objects are not “lost.” The consistent tracking

coverage assures consistent measurements that can be used to characterize the object properties and dynamics. The baseline OD process uses the Goddard Trajectory Determination System (GTDS) orbit determination tool which implements a batch least-squares approach to estimating the state of each high A/m object. The estimated state consists of position and velocity information, and a solar radiation coefficient “factor” that effectively estimates a measure of the area-to-mass ratio.

In addition to earth, lunar and solar gravitation, the solar radiation pressure (SRP) is a significant force affecting the orbital dynamics of GEO objects. Objects having high area-to-mass ratio are particularly susceptible to solar force acceleration. The solar radiation acceleration is [4]

$$\bar{a}_{radiation} = \frac{p_{SR} c_R A_S}{m} \hat{r}_S \quad (1)$$

where

p_{SR} = solar radiation pressure

c_R = reflectivity coefficient

A_S = effective area facing sun

m = object mass

\hat{r}_S = unit vector from object to sun

In most OD implementations a nominal value of c_R is typically specified, and a fixed correction estimated as part of the batch least squares state solution. The values of A_S and m are usually specified if those properties are known, and the values of p_{SR} and \hat{r}_S are computed based on the orbital geometry relative to the sun. In the absence of physical information of the object properties, the combined quantity of

$$\gamma = \frac{c_R A_S}{m} \quad (2)$$

can be estimated. If $c_R = 1$, then we are effectively estimating the area-to-mass ratio. For the GTDS batch least square implementation, the A/m is estimated as a constant over the fit span. This limitation can have a significant effect if A/m varies significantly over the time scale of the fit span. Note that mass is assumed fixed, and so A/m variations are really just an indication of the object orientation changes resulting in variation of the cross sectional area exposed to the sun.

The batch least-squares OD process strategy is illustrated in the process diagram of Fig. 3. Either a TLE, or state vector in any specified format, can be used to derive an *a priori* state vector. With a fit span specified, the data are used to estimate a state near the end of the fit span. That estimated state is propagated using appropriate force models to a predicted future time. Because some observing systems require a TLE be used in the acquisition process, the prediction process also derives TLEs at nominal 1-day intervals from the predicted osculating state. In this implementation, the end of a predicted state derived from a previous estimate can be used as the *a priori* state for the next estimate. This implementation is flexible enough to allow variable fit spans to accommodate the possible time variations of the area-to-mass factor. Creating the TLEs at 1-day intervals helps to mitigate the SGP4 propagation error contribution to the overall error. Both osculating state vectors and TLEs, along with OD fit metrics, will be provided to collaborators for use in acquiring high A/m objects that are tracked by AFSPC.

Notes:

- Data span for OD update not a fixed interval – data tracking dependent
- The propagation span is fixed – nominally 2 weeks
- State vector written at fixed interval – nominally 1 day
- OD initial state taken from closest propagation state
- Updated TLE's derived from propagated state vectors

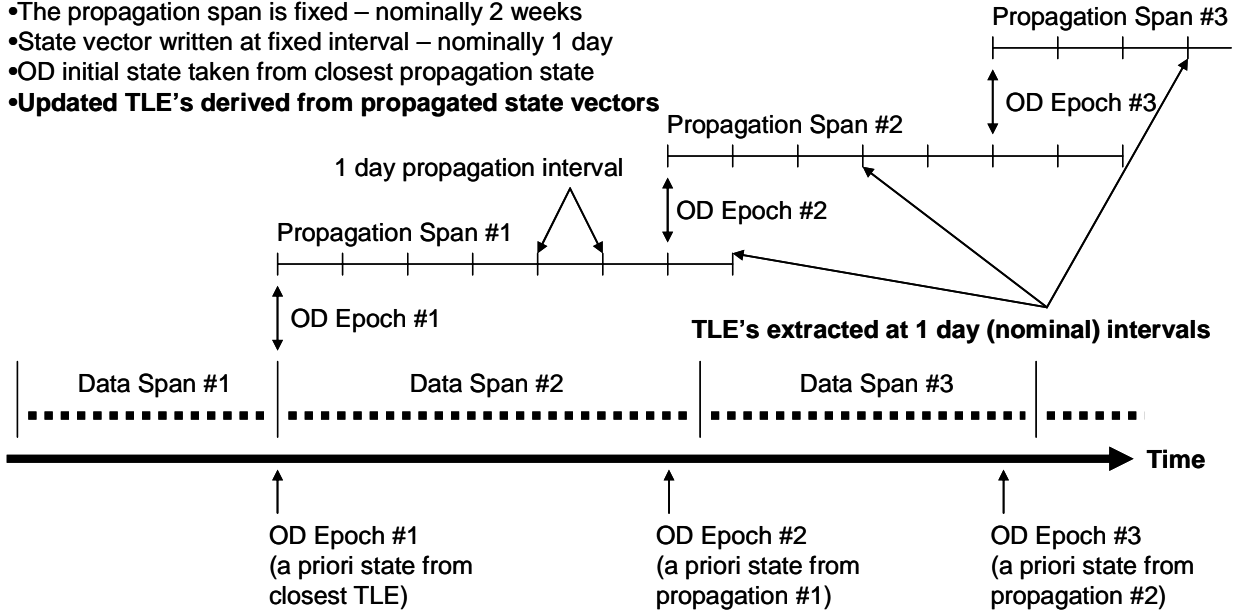


Fig. 3. Batch Orbit Determination Processing Strategy

The Orbit Determination Tool Kit (ODTK) was also used to examine a “real-time” implementation of the state estimation. It has the capability to provide insight into the dynamics that might occur over a fit span. In particular, the potential time variability of the A/m parameter is of interest. ODTK utilizes a Kalman filter based approach to the estimation, and so a state estimate is provided at each measurement update, hence, a time history of each estimated parameter is available. Furthermore, the filtered state can be smoothed “backwards” over a specified data span to provide an optimal state estimate that reduces the uncertainty over that produced by the real-time filter. The filter parameters are saved after the latest update, and so after a measurement outage, the state is automatically propagated to the new measurement time, and proceeds with the filter update as long as data from a pass is available. Most noteworthy is that the ODTK Kalman filter implementation allows A/m to be estimated with each measurement update, and so characterization of the time history is possible. This will be illustrated in the results presented in the next section.

4. DATA PROCESSING AND ORBIT DETERMINATION RESULTS

The batch least squares processing was problematic for some of the data that was analyzed, and so the process is still being refined. The chief factor appears to be variations in the A/m; the batch process only allows estimation of the A/m as a fixed parameter, so a strategy that accommodates the variation needs to be incorporated into the OD selection of the fit span. No effort was made to “optimize” the fit spans for any of the objects, though this will be dependent somewhat on the available tracking and physical behavior of the object of interest. Debris having high A/m characteristics typically has unpredictable orientation dynamics and, hence, unpredictable A/m. For this initial work the fit spans were selected based on trial and error in attempt to find a fit span the produced converged solutions with residuals 10’s of arc-seconds or less.

Performance metrics from the GTDS OD batch process results are summarized in Table 2 for each of the 6 trial objects. All objects had fit spans of 9-10 days, except for Obj#6 which had 19. The RSS values represent the total position and velocity adjustments of the state at the epoch time relative to the a priori reference state. The a priori reference state was derived from TLEs provided by AFSPC which did not necessarily correspond to the epoch time, though the process attempts to pick the TLE with the epoch closest to the desired OD epoch. The RSS position adjustments range from 10’s to 100’s of km, which is reasonable considering the expected TLE accuracies and the differences between the TLE and OD epoch times. The post-fit residuals range from fractions to 10’s of arc-

seconds, the higher values indicating the possibility of un-modeled errors. Finally, the A/m adjustments range from ~1% to ~86% of the nominal values. The higher adjustment values seem to correspond to the higher residuals, implying the possibility of A/m modeling deficiencies. The ODTK A/m estimation results are shown in Fig. 4 for Obj#6, and show A/m variations of similar magnitudes to that shown in Table 2. Note that the ODTK estimate is the correction to the nominal value of 3.4801 m²/kg.

OBJ#	A/m (m ² /kg)	Fit Span (Days)	RSS Pos Δ (km)	RSS Vel Δ (m/s)	%Δ Nom A/m	AZ Res Bias (as)	AZ Res Sig (as)	EL Res Bias (as)	EL Res Sig (as)
4	13.0619	10	139.3531	9.7107	1.5000	-0.0919	1.7415	-0.0009	0.6566
5	2.2836	10	448.1207	26.1544	35.1491	0.5364	4.5972	-0.0658	1.3187
6	2.2218	19	844.9701	48.8494	86.6307	-0.1978	7.5689	-0.2135	3.4801
7	1.0191	9	96.1723	5.6033	4.7704	-4.1622	18.3002	0.6927	5.2707
8	5.7977	10	68.4375	3.9515	16.2971	7.5395	24.7666	-0.5019	8.7236
9	2.0179	9	90.5648	6.4177	1.1052	-0.1432	4.2299	-0.1074	0.9559

Table 2. GTDS OD Performance Summary for Trial High A/m Objects

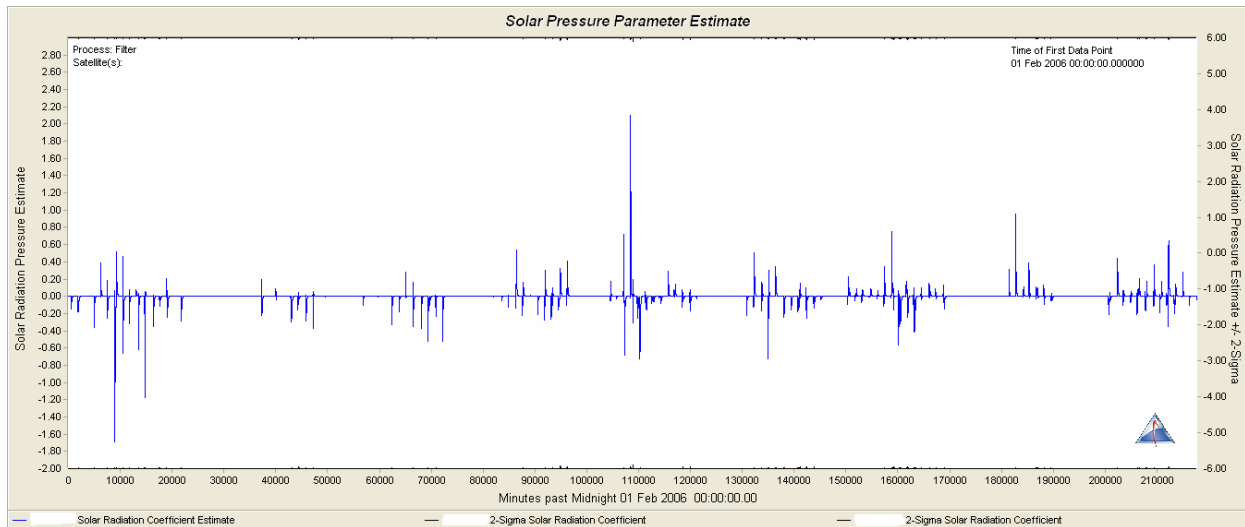


Fig 4. ODTK A/m Correction Estimates for Obj#6 (152 day span)

No reference orbits were available for any of the trial objects, and hence, no “true” orbits were available to assess prediction performance. Prediction accuracy is a function of many factors, including measurement quality, quantity, frequency and observation geometry, the method and fidelity of the propagation, and the fidelity of the forces modeled versus actual forces. Acquisition tests using prediction products resulting from the OD process will help to quantify the accuracy.

The TLEs derived from the GTDS process were compared to “references” derived from the osculating state vectors. The pointing comparisons are provided in Table 3, and are the maximum pointing and pointing rate errors that would result from a Maui observer. All of these pointing errors are much less than the 40 arc-minutes required for acquisition by typical optical observing systems, though this is really just a measure of the SGP4 fidelity over the 24 hour propagation span, and not of overall absolute accuracy. It should be noted that SGP4 does not include solar radiation pressure effects, and so this limitation is likely reflected in some of the differences. As previously mentioned, no effort was made to “optimize” the fit spans, and so this discrepancy is exacerbated by inadequate A/m modeling.

OBJ#	A/m (m ² /kg)	Ra Ptg Δ (arcmin)	Dec Ptg Δ (arcmin)	Ra Rate Δ (arcmin/hr)	Dec Rate Δ (arcmin/hr)
4	13.0619	3.0	2.5	0.5	0.5
5	2.2836	3.0	2.0	1.0	1.0
6	2.2218	2.5	0.5	0.5	0.5
7	1.0191	3.5	1.0	0.5	0.5
8	5.7977	9.0	3.0	1.5	1.0
9	2.0179	10.0	2.5	2.0	1.0

Table 3. Max Pointing Errors from Maui: GTDS vs. Reference TLEs

Another measure of prediction accuracy can be gleaned from the Kalman filter state vector adjustments that occur whenever an observation update occurs after a period of measurement outage, as the filter must propagate the state based on the estimate at the previous measurement to the time of the new measurement. For a “tuned” filter, these state adjustments are consistent with the propagated state covariance. Fig. 5 shows the radial, in-track and cross-track (RIC) smoother covariance for Obj#6, while Fig. 6 shows the corresponding positional adjustments at update times. Note that position differences are consistent with the batch least-squares adjustment given in Table 2.

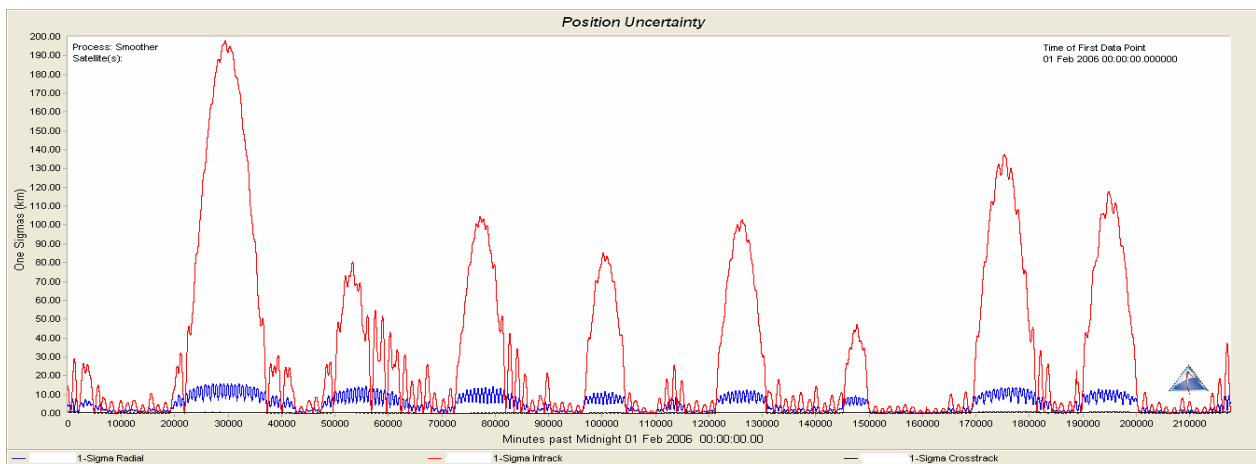


Fig 5. ODTK A/m RIC Smoother Covariance for Obj#6 (152 day span)

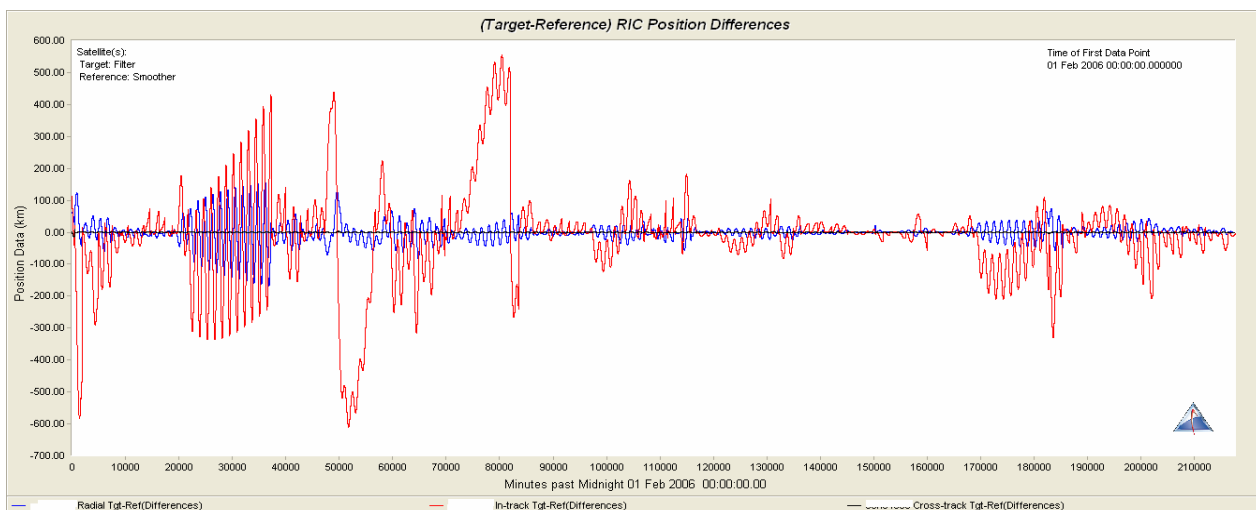


Fig 6. ODTK A/m RIC Position Adjustments for Obj#6 (152 day span)

5. CONCLUSIONS AND FUTURE WORK

The OD results for angles-only observations demonstrate one of the challenges for the OD and orbit prediction of high A/m objects. In particular, the ODTK Kalman filter results clearly show the correlation between the inherently poor radial component resolution and the along-track orbit error (drift). This might be mitigated somewhat by observations taken from geographically diverse observational sites. Also noteworthy from the ODTK results is the apparent time variations of the A/m value. It is plausible that this is real, as it is consistent with the physics of an object whose orientation with respect to the sun vector varies over time. If these variations prove to be periodic and can be characterized, they can potentially be modeled and used to improve the orbit prediction performance. A chaotic behavior would have a noise-like affect of diminishing the orbit prediction performance.

At the time of this writing, tests are being conducted to further validate and refine the OD and orbit prediction process through a series of observational tests. Predictions derived from the OD results will be used in an attempt to acquire some of the trial objects using MSSS resources. The trial object orbits must be phased such that the object is within view from Maui in order to be acquired, but they must also have a visual magnitude compatible with the sensitivity of the MSSS sensors. Weather and lighting conditions must also be favorable. If successfully acquired, the acquisition offsets of the acquired objects can be compared to the predicted acquisition pointing as a measure of performance. Other tests will consider handoffs between sensors, both between MSSS sensors and between MSSS and other (off-island) sensors. Some efforts will also include attempts to quantify and validate the time variations of the SRP A/m, and possibly use them in an attempt to improve the orbit prediction performance.

6. REFERENCES

1. Schildknecht et al., Properties of the High Area-to-mass Ratio Space Debris Population in GEO, AMOS Tech. Conf. 2005.
2. Kelecy, T. and C. Sabol, "Rapid Orbit Characterization and Real-time State Vector Handoff Using High Accuracy Metrics," AMOS Conference Proceedings, Kihei, HI, September 2004.
3. Musci, R., T. Schildknecht and M. Ploner, Orbit improvement for GEO objects using follow-up observations, Advances in Space Research 34 (2004) 912-916 (COSPAR), 2004.
4. Vallado, David A., "Fundamentals of Astrodynamics," Second Edition, Microcosm Press, 2001.

7. ACKNOWLEDGEMENTS

This research would not have been possible without the NASA JSC and the U.S. Space Command. A special thanks goes to Robin Thurston of the 1st Space Control Squadron (1 SPCS) for providing the observational data.